AUSTENITE AND FERRITE GRAIN SIZE EVOLUTION IN PLAIN CARBON STEEL

M. Militzer, A. Giumelli, E. B. Hawbolt and T.R. Meadowcroft

The Centre for Metallurgical Process Engineering, University of British Columbia

Vancouver, B.C., Canada V6T 1Z4

ABSTRACT

Grain size evolution in a 0.17%C, 0.74%Mn plain carbon steel is investigated using a Gleeble 1500 thermomechanical simulator. Austenite grain growth measurements in the temperature range from 900 to 1150°C have been used to validate the Abbruzzese and Lücke model, which is recommended for simulating grain growth during reheating. For run-out table conditions, the ferrite grain size decreases from 11μm to 4μm when the cooling rate from the austenite is increased from 1 to 80°C/s.

1. INTRODUCTION

During recent years, microstructure engineering in hot strip mills has gained significant attention with the goal being to develop a predictive tool which quantitatively links the processing parameters to the properties of the hot-rolled steel product. For low carbon steels, mechanical properties such as strength and toughness can be directly related to the ferrite grain size developed as a result of the thermomechanical treatment. During rolling, austenite grain growth is the dominant process in reheating and delay between rough and finish rolling. The austenite grain size and shape results mainly from the conditions imposed by recrystallization and precipitation. The austenite microstructure after rolling and the cooling conditions on the run-out table determine finally the ferrite grain size.

To get the required quantitative link between process parameters and resulting grain size numerous studies of austenite and ferrite grain growth kinetics have been performed and empirical relations have been proposed [1-5]. However, the extrapolation of such empirical relations to industrial conditions remains questionable since the thermomechanical treatment employed in an experiment is usually considerably different from the mill situation. Moreover, such relations are based on the measurements of two-dimensional microstructures, virtually neglecting the three-dimensional character of the grains. Therefore, it is important to determine the actual volumetric grain size from the two-dimensional measurement and to explore the mechanisms of the experimentally observed grain size evolution. It should be possible to extrapolate with confidence, a model based on these mechanisms to the mill conditions.

DISCLAIMER

The present paper reports an attempt to develop an improved description of the grain size evolution in a plain carbon steel, where austenite and ferrite grain growth have been investigated. The method of Takayama et al. [6] to estimate the three dimensional grain size distribution is critically analyzed. Austenite grain growth kinetics are described in terms of the statistical grain growth model of Abbruzzese and Lücke [7]. On the basis of this model, a pinning parameter is determined and extrapolated to the condition of the delay between rough and finish rolling. The cooling rate dependence of the ferrite grain size is investigated for run-out table cooling conditions. Recrystallization kinetics of the given steel is discussed in a second paper [8].

2. EXPERIMENTAL MATERIAL AND METHODOLOGY

An industrial plain carbon A36 steel was investigated which had been received from the Gary works of US Steel. Its chemical composition is listed in Table I in weight percent. All heat treatments were performed employing the GLEEBLE 1500 thermomechanical simulator. Tubular specimens with a length of 20mm, an inner diameter of 6mm and a wall thickness of 2mm were machined from the as received steel plates for austenite grain growth tests; a wall thickness of 1mm was used for ferrite grain growth tests.

Table I. Chemical Composition of the A36 Steel (wt%)

C	Mn	P	S	Si	Cu	Ni	Cr	Al	N
0.17	0.74	0.009	0.008	0.012	0.016	0.010	0.019	0.040	0.0047

The following austenite grain growth tests were performed:

1. Isothermal tests at 950, 1000, 1050, 1100 and 1150°C with an initial heating rate of 5°C/s.
2. Stepped isothermal tests by initially heating the sample to 900°C at 5°C/s, holding for 120s and rapidly heating (100°C/s) to and holding at 1050 and 1100°C.
3. A continuous cooling test by initially heating the sample to 900°C at 5°C/s, holding for 120s and rapidly heating (100°C/s) to 1120°C, then cooling at 2°C/s to 1000°C to simulate the delay between rough and finish rolling.

After the heat treatment, the specimens were quenched to obtain a final microstructure, which allowed the identification of the prior austenite boundaries. Two quench regime were employed.

For larger grain sizes above 60 μm, the samples were He quenched; by regulating the cooling rate via the He flow rate, a ferrite fraction of approximately 5% was obtained outlining the austenite boundaries. For smaller grain sizes, the samples were quenched more rapidly with water to obtain a martensitic microstructure, where the austenite boundaries were revealed by etching.

To determine the effect of cooling rate from the austenite on the resulting ferrite grain size, specimens were heated at 5°C/s to 950°C, where they were held for 120s. They were then cooled at 1°C/s to 900°C and held there for an additional 120s. After this standardized pre-heating schedule, the continuous cooling test was performed applying the appropriate cooling regime spanning the run-out table conditions. Three types of cooling procedures were employed: controlled cooling for low cooling rates (<10°C/s), air cooling (cooling rate of approximately 15° C/s) and He cooling for higher cooling rates, where the He flow was varied to obtain a range of cooling rates extending from 30 to 250°C/s. In some additional tests, the samples were cooled to 600°C and held there for one hour to assess potential ferrite grain growth as experienced during coiling.

The resulting grain size was measured employing the area method (Jeffries procedure) [9] yielding the mean area , A, from which the equivalent area diameter (EQAD), d_A, is defined by

$$d_A = \sqrt{\frac{4A}{\pi}} \qquad (1)$$

The grain size distribution was determined based on area measurements with the Electron Optics System (EOS) image analyzing system. In addition, the austenite grain size was measured with the linear intercept method (Heyn procedure) [9] yielding the mean linear intercept, l.

3. CONSTRUCTION OF THE SPATIAL DISTRIBUTION

All these methods are based on measurements obtained from a two-dimensional micrograph of the three dimensional sample. Thus, the results do not give the spatial grain size distribution which is actual of interest. Since it is very time consuming to determine the latter directly, a number of attempts have been made to construct the spatial distribution from two-dimensional measurements. In general, such approaches assume a spherical grain shape, which does not allow for space filling [10,11]. As a consequence, some doubtful results, e.g., negative grain numbers, are obtained for the spatial distribution constructed in this way. However, Takayama et al. [6] have recently proposed a method to construct the spatial distribution from the two-dimensional standard measurements under the assumption that the spatial distribution is log

normal and the grain shape is the tetrakaidecahedron. The latter allows for space filling, whereas the former is characteristic for normal grain growth. Employing this method, first the log normality of the grain size distribution has to be confirmed with measurements of the two dimensional distribution, e.g. as obtained from area measurements using an image analyzer. Then the mean linear intercept, l, and mean area, A, are determined according to the standard methods [9].

The log normal distribution [12]

$$f(d) = \frac{1}{(2\pi s^2)^{1/2} d} \exp\left(\frac{-\ln(d/d_g)}{2s^2}\right) \tag{2}$$

is characterized by the peak grain size value, d_g, and the standard deviation, s. These parameters are related to the measured l and A according to Takayama et al. [6] by

$$l = 0.60661 d_g \exp(5s^2/2) \tag{3}$$

and

$$A = 0.4861 d_g^2 \exp(4s^2) \tag{4}$$

Thus, the measurement of l and A provides the required information to construct the spatial distribution with the help of equations (3) and (4). Further, the average grain size of the three-dimensional distribution is given by

$$D = d_g \exp(s^2/2) \tag{5}$$

and the mean volumetric grain size by

$$d_m = d_g \exp(3s^2/2) \tag{6}$$

The latter is the relevant grain size, since it actually represents the diameter of a grain with the average grain volume.

4. AUSTENITE GRAIN GROWTH

4.1. Experimental results

For each test, the number of grains measured is in the range 200-500. The average experimental error in determining l and A, respectively, is approximately 10%. Figure 1 shows the results of isothermal grain growth when the heating rate, ϕ, to the measurement temperature is 5°C/s. The initial EQAD is approximately 15μm for T<1050°C and above 80μm for T>1050° C, indicative of substantial grain growth occurring during heating to the higher temperatures. This rapid grain coarsening can be attributed to abnormal growth processes which are related to coarsening and dissolution of AlN particles. Abnormal growth is observed in the range 950 to 1050°C; for a holding time decreasing from 600s at 950°C to 10s at 1050°C, a non-homogeneous microstructure develops in which areas of fine grains are embedded in regions of substantially larger grains. The fine grain areas eventually disappear and normal growth of the coarser grains takes place. The two-dimensional grain size distribution is shown in Figure 2 for two holding times at 1150°C. The results support the log normality of the distribution, which is characteristic for normal grain growth. Figure 3 shows the grain growth kinetics for the stepped isothermal tests employing rapid heating from 900 to 1100°C. This stepped heat treatment procedure reduces the effects of abnormal grain growth significantly. The non-homogeneous microstructure is initially observed but disappears after a few seconds. The initial EQAD of the larger grains is approximately 50μm and normal growth of these grains is observed. As for the tests with slower heating rates, a limiting grain size is approached after approximately 120s, but is substantially smaller for the rapid heating tests. The limiting EQAD decreases from 140 to 100μm at 1100°C and from 115 to 85μm at 1050°C, respectively. The solid lines in Figs. 1 and 3, respectively, represent the conventional empirical description using the power law

$$d_A^m = d_{A,0}^m + K_o \exp(-Q/RT)t \qquad (7)$$

where the growth exponent, m, the apparent activation energy, Q, and K_o are the fitting parameters. Table II summarizes the three sets of these parameters used to obtain the lines shown in Figs. 1 and 3.

Table II. Empirical Parameters for the Grain Growth Power Law

Series	m	Q/kJmol^{-1}	K_o/μm^{m}s^{-1}
ϕ=5°C/s (fine grains)	3.4	1291	1.51×10^{47}
ϕ=5°C/s (coarse grains)	8.2	840	5.46×10^{54}
ϕ=100°C/s	14.9	1089	1.94×10^{68}

In the continuos cooling test designed to simulate the delay between rough and finish rolling, no sign of abnormal growth has been observed presumably due to the somewhat higher initial temperature of 1120°C, where the EQAD is approximately 50μm. Rapid grain growth occurs at the higher temperatures and the growth rate quickly decreases, as illustrated in Figure 4. The EQAD at 1000°C is 71μm. This is a substantially smaller grain size than is obtained under mill conditions, where an EQAD of approximately 160μm is observed, despite the fact that the initial EQAD of 50μm is in the range readily expected as the grain size of recrystallized austenite after rough rolling.

Since the grain size distribution is log normal for normal grain growth (cf. Figure 2), Takayama's method to determine the spatial distribution is applicable for austenite grain growth at the higher temperatures of interest. Because of the sensitivity of the standard deviation, s, to the experimental error of the measured l and A, an unreasonable scatter of s occurs. However, the mean value of s is for each isothermal tests approximately 0.3. Thus s=0.3 is employed to estimate the spatial distribution, which is, to first approximation, equivalent to the following relations between the measured values and the mean volumetric diameter

$$d_m = 1.2 d_A = 1.5 l \qquad (8)$$

It should be emphasized that these relationships have to be viewed with care since they are based on a method which is applicable only to normal growth and a uniform single grain shape. The large experimental scatter of s (0.03-0.49) further indicates the limitations of this method in estimating the actual spatial distribution.

4.2. Modeling

The statistical grain growth model of Abbruzzese and Lücke [7] is employed to predict the grain growth kinetics. In this approach a pinning parameter accounts for the characteristic inhibition of normal grain growth due to precipitates and solute drag, respectively. The basic assumptions and equations of the model are as follows. The actual grain structure is replaced by a spherical grain structure with equal grain volume. The grain size distribution, $f(R)$, can be subdivided logarithmically into n grain size classes. Then, growth or shrinkage of a grain of size class, i (grain radius R_i), is considered under the assumption that it is surrounded statistically by grains of all other size classes. Provided size i is sufficiently greater than size j, a driving force $F_{ij} > 0$ exists and grain i tends to consume neighboring grain j, where

$$F_{ij} = \gamma_{gb}\left(\frac{1}{R_j} - \frac{1}{R_i} - P\right) \tag{9}$$

Here, γ_{gb} is the grain boundary energy and P is related to the pinning force, F_P, by $P=F_P/\gamma_{gb}$. The following relationships hold for the driving forces: $F_{ij}=-F_{ji}$, and $F_{ij}=0$ if $F_{ij}<0$ for $R_i>R_j$. The growth (or shrinkage) rate of a grain with size i is

$$\frac{dR_i}{dt} = M_{gb}\sum_j w_{ij} F_{ij} \tag{10}$$

The grain boundary mobility, M_{gb}, is approximated with the grain boundary diffusion, D_{gb}, by

$$M_{gb} = D_{gb} b^2 / kT \tag{11}$$

where b is the magnitude of the Burgers vector. The probability, w_{ij}, that grains i and j are neighbors, is given for a random distribution by

$$w_{ij} = \frac{f_j R_j^2}{\sum_j f_j R_j^2} \tag{12}$$

where $f_j=N_j/N_{tot}$ represents the fraction of grains with size j. Here, N_j is the number of grains per unit volume in class j and N_{tot} is the total number of grains per unit volume. The change in the

grain size distribution is then calculated per time step leading to the prediction of the grain size evolution. The model was further extended to account for non-isothermal conditions.

4.3. Prediction of the pinning force

This model is applied to the grain growth kinetics in the A36 steel employing γ_{gb} = 0.7Jm^{-2} [13] and D_{gb}=0.89cm^{2}s^{-1}exp(-1.66eV/kT) [14]. Using P as a fitting parameter, good agreement with the experimental results has been achieved, as shown in Figure 5 by the solid lines. The pinning parameter decreases with temperature and increases with heating rate, as illustrated in Figure 6. For ϕ=5°C/s, a linear increase of P with temperature (in K) is confirmed

$$P = -80m^{-1}(T - 1511) \tag{13}$$

Zener [15] proposed an expression for pinning related to the presence of particles:

$$P = \frac{3\nu}{4r} \tag{14}$$

where ν is the volume fraction of particles and r the mean particle radius. Assuming that r for AlN is in the range 5 to 10nm [16], the predicted P corresponds to reasonable values of ν in the order of 10^{-5}-10^{-4}. These are similar results as obtained for an analysis of grain growth in a 1080 eutectoid, Al-killed, plain carbon steel [17]. As illustrated in Figure 7, P also compares favorably to Zener's criterion for the limiting grain radius

$$R_{lim} = P^{-1} \tag{15}$$

where the grain size, which is measured after the longest holding times, can be taken as an indication of the limiting grain size.

The isothermal test results underscore that the heat treatment schedule, e.g. different heating rate, ϕ, can have a considerable effect on the successive grain growth behavior. Such behavior can be attributed to related variations of the volume fraction, ν, and the radius, r, of the precipitates. Consequently, it is not surprising that the continuous cooling test designed to simulate the grain growth obtained during the delay by cooling from 1120 to 1000°C at 2°C/s (total 60s) after rapid heating from the austenitizing temperature of 900°C resulted in a much smaller grain size than that observed under mill conditions. In the latter case, the material is reheated for several hours at approximately 1300°C, allowing AlN particles to dissolve, followed by rough rolling above the solution temperature of AlN. Re-precipitation of AlN during cooling,

a comparatively slow process [18], is expected to take place in the A36 steel below 1000°C. Thus, austenite grain growth during the rougher to finisher delay in the mill is not inhibited by the presence of AlN, whereas in the continuous cooling test, a significant number of AlN particles are expected to have survived the rapid heating. The observed grain growth kinetics is consistent with the Abbruzzese-Lücke model assuming P=20mm^{-1}, which is indicated by the corresponding isothermal tests.

Employing the Abbruzzese-Lücke model, the effective pinning parameter for delay in the mill (cooling from 1120 to 1000°C in 60s) was estimated. Taking the recrystallized grain size after roughing to be 50-70μm, marginal pinning, i.e. $P\approx 0$, is required to obtain the observed grain coarsening with an average grain size, D, of approximately 180μm before finishing. This is indicative of unpinned austenite grain growth taking place in the Al killed plain carbon steels when recrystallization is completed after each rough rolling pass. During finish rolling with interstand times decreasing from a few seconds to a fraction of a second, grain growth appears to be of minor importance, independent of the pinning degree. Unpinned growth is described by [19]

$$\frac{dD}{dt} = \frac{K}{2D} \tag{16}$$

where the growth constant, K, can be expressed as a function of γ_{gb} and M_{gb}. Since the grain boundary energy, γ_{gb}, increases with decreasing carbon content because of reduced carbon grain boundary segregation [13], K is expected to increase accordingly. On the other hand, the temperature dependence of K is mainly determined by the grain boundary diffusivity (cf. equation (11) for M_{gb}).

5. FERRITE GRAIN SIZE

Table III summarizes the results of the EQAD of the ferrite grains, $d_{\alpha A}$, obtained after continuous cooling tests in which the austenitizing temperature was 950°C, and the initial mean volumetric austenite grain size was 18μm. This small grain size was used to simulate the austenite grain size in the final stages of finish rolling, prior to run-out table cooling and coiling. The cooling rate, φ, at 850°C, the temperature where 5% of austenite is transformed into ferrite, $T_{0.05}$, and the final ferrite fraction , F, are included in this Table. In each test, 400 - 800 grains have been measured to obtain reliable mean values. The results of the additional tests, where the cooling was interrupted for one hour at 600°C, are not included in this Table, since such a

modified cooling regime did not change the ferrite grain size; these results suggest that negligible ferrite grain growth should occur during coiling at temperatures near 600°C.

Table III. Experimental Results of Ferrite Grain Size Measurements

φ, °C/s	$T_{0.05}$, °C	F	$d_{\alpha A}$, μm
1	752	0.80	10.9
5	743	0.82	9.0
19	731	0.77	7.7
41	718	0.80	6.3
58	702	0.77	4.6
79	700	0.77	4.1

The measured ferrite grain size distribution is shown for two cooling rates in Figure 8. For φ=41°C/s, severe deviations from the log normality are evident, whereas for φ=58°C/s the distribution appears to be log normal. Since the ferrite grain size distribution is a result of the austenite-to-ferrite transformation during cooling rather than of normal grain growth, deviations from log normality cannot be neglected and Takayama's method to estimate the spatial distribution is in general not applicable. In a later stage of this study, it is intended to employ as an alternative the method developed by Matsuura and Itoh [20] to estimate the three dimensional distribution from the measured one. The Matsuura-Itoh method is more general and does not require the distribution to be log normal. Twelve types of polyhedra are employed to describe the variety of grain shapes in the actual material and no further assumptions are made.

Figure 9 shows the final ferrite grain size as a function of cooling rate. Grain refinement occurs with increasing cooling rate. The results can be described by an empirical relation of the type

$$d_{\alpha A} = B\varphi^{-q} \tag{17}$$

with B=11.37μm(°C/s)^q and q=0.18, as shown by the solid line. Choquet et al. [5] propose a similar relationship with q=0.17 and B is a function of chemical composition and the initial austenite grain size, d_γ

$$B = (5.76 - 10C - 1.3Mn)d_\gamma^{0.45} \tag{18}$$

The dashed line in Figure 9 gives the prediction for the A36 steel according to Choquet's relation leading to a similar agreement for all cooling rates. Interestingly, a relationship of type (17) with q=0.17, was also obtained from theoretical considerations by Tamura [21]. However, the fit with equation (17) is not completely satisfying for the higher cooling rates (>20°C/s), which are important for the accelerated cooling experienced on a run-out table.

Figure 10 gives an alternative representation of the final ferrite grain size, which is shown as a function of $T_{0.05}$, the temperature where 5% ferrite has been formed indicative for the transformation start. Following the empirical approach of Suehiro et al. [22], the solid line

$$d_{\alpha A} = \{\beta \exp(-E / T_{0.05}) F\}^{1/3} \tag{19}$$

gives the best fit to the experimental data with β=7.38×10^{24} and E=51155 when $T_{0.05}$ is taken in K. The agreement with the experimental results is excellent for all cooling rates. For comparison, the relation of Suehiro et al.

$$d_{\alpha A} = \{5.51\times10^{10} d_{\gamma}^{1.75} \exp(-21430 / T_{0.05}) F\}^{1/3} \tag{20}$$

which was reported for plain carbon steels (0.1-0.15wt%C, 0.5-1.5wt%Mn) containing 0.5wt%Si is shown by the dashed line in Figure 10. Equation (20) predicts values which are about 7μm bigger than those measured in the present study. The differences could be attributed to the different chemistry (Si content) and metallic inclusion content in the two steels.

6. CONCLUSIONS

1. For microstructural engineering, it is important to have information on the actual volumetric grain size. The method of Takayama et al. was employed to estimate the spatial grain size distribution from the measured two-dimensional one. This method appears to be applicable only in a limited number of cases for austenite grain growth, where normal growth is dominant. Therefore, it is suggested to further investigate the more general method of Matsuura and Itoh to determine the spatial distribution. This approach will also allow comparison with the results obtained by Takayama's method for normal growth.

2. Austenite grain growth kinetics in the A36 steel depend strongly on the pre-heating schedule which controls the presence/absence of AlN precipitates, and their effect on grain

boundary movement. The effective pinning force can be estimated with the statistical grain growth model of Abbruzzese and Lücke. Whereas significant pinning is confirmed for the experiments, austenite grain growth in a hot strip mill before finishing, can be expected to occur unpinned for plain carbon steels. In microalloyed grades, pinned growth may also occur under mill conditions, particular when the steel contains Ti, since TiN usually does not completely dissolve during reheating. The Abbruzzese-Lücke model is recommended for simulating the grain growth obtained during reheating and the delay time between the roughing and finishing mill; empirical relations found in conventional grain growth tests can only be used with extreme care.

3. The final ferrite grain size of the A36 steel hot rolled at the USS Gary works is approximately 6μm, a grain size which was obtained in the tests by employing a cooling rate of 41°C/s. As a predictive tool, it is suggested to use Suehiro's method of representing the ferrite grain size as a function of ferrite fraction and transformation start temperature rather than cooling rate.

ACKNOWLEDGMENT

The authors appreciate the financial support received from the American Iron and Steel Institute (AISI) and the Department of Energy (DOE). The assistance of B. Chau performing the GLEEBLE tests and R. Cardeno performing quantitatively metallography is gratefully acknowledged.

REFERENCES

1. C.M. Sellars and J.A. Whiteman, *Met. Sci.*, 187 (1979).
2. E. Anelli, *ISIJ International* **32**, 440 (1992).
3. P.D. Hodgson and R.K. Gibbs, *ISIJ International* **32**, 1329 (1992).
4. S. Licka and J. Wozniak, *Kovove Mater.* **20**, 562 (1982).
5. P. Choquet, P. Fabregue, J. Giusti, B. Chamont, J.N. Pezant and F. Blanchet, *Mathematical Modelling of Hot Rolling of Steels*, 34 (CIMM, Hamilton, 1990).
6. Y. Takayama, N. Furushiro, T. Tozawa, H. Kato and S. Hori, *Mat. Trans. JIM* **32**, 214 (1991).
7. G. Abbruzzese and K. Lücke, *Mat. Sc. Forum* **94-96**, 597 (1992).
8. W.P. Sun and E.B. Hawbolt, this issue.
9. Annual Book of ASTM Standards, Vol., E112

10. S.A. Saltykov, *Stereology* (H. Elias ed.), 163 (Springer, New York, 1967).
11. K.P. Huang and W. Form, *Prakt. Met.* **27**, 332 (1990).
12. S.K. Kurtz and F.M.A. Carpay, *J. Appl. Phys.* **51**, 5725 (1981).
13. N.A. Gjostein, H.A. Domian, H.I. Aaronson and E. Eichen, *Acta metall.* **14**, 1637 (1966).
14. H.J. Frost and M.F. Ashby, *Deformation-Mechanism Maps*, 60 (Pergamon Press, Oxford, 1982).
15. C. Zener, private communication to C.S. Smith, *Trans. Metall. Soc. AIME* **175**, 15 (1948).
16. G. Wang, "Static Recrystallization and Precipitation in Nb-Al HSLA Steels", (Ph.D. thesis, McGill University, Montreal, 1990).
17. M. Militzer, W.P. Sun, E.B. Hawbolt and J.J. Jonas, *Advances in Hot Deformation Texture and Microstructures* (eds. J.J. Jonas, T.R. Bieler and K.J. Bowman), 157 (TMS, Warrendale, 1994)
18. T. Gladman and F.B. Pickering, *J. Iron Steel Inst.* **205**, 653 (1967).
19. J.E. Burke and D. Turnbull, *Prog. Metal. Phys.* **3**, 220 (1952).
20. K. Matsuura and Y. Itoh, *Mat. Trans. JIM* **32**, 1042 (1991).
21. I. Tamura, *Trans. ISIJ* **27**, 763 (1987).
22. M. Suehiro, K. Sato, Y. Tsukano, H. Yada, T. Senuma and Y. Matsumura, *Trans. ISIJ* **27**, 439 (1987).

APPENDIX: NOMENCLATURE

A	mean grain area
b	Burgers vector
B	fitting parameter for ferrite grain size dependence on cooling rate
d_A	equivalent area diameter
$d_{A,0}$	initial equivalent area diameter
$d_{\alpha A}$	equivalent area diameter of ferrite grains
d_g	peak grain size value of log normal distribution
d_m	mean volumetric grain size
d_γ	austenite grain size before γ-α transformation
D	average grain size of three-dimensional distribution
D_{gb}	grain boundary diffusivity
E	fitting parameter for ferrite grain size as function of transformation start
f	grain size distribution
f_i	fraction of grains of size i
F	final ferrite fraction
F_{ij}	driving force for grain growth between grains of size i and j
F_P	pinning force
k	Boltzmann constant

K	grain growth constant
K_o	fitting parameter in grain growth power law
l	mean linear intercept
m	grain growth exponent
M_{gb}	grain boundary mobility
n	number of grain size classes
N_i	number of grains per unit volume in size class i
N_{tot}	total number of grains per unit volume
P	pinning parameter
Q	apparent activation energy of grain growth (power law)
r	average particle radius
R	gas constant
R_i	radius of grain of size i
R_{lim}	limiting grain radius
s	standard deviation of log normal grain size distribution
t	time
T	temperature
$T_{0.05}$	transformation start temperature
w_{ij}	probability that grains i and j are neighbors
β	fitting parameter for ferrite grain size as function of transformation start
γ_{gb}	grain boundary energy
ϕ	heating rate
φ	cooling rate
ν	volume fraction of precipitates

Figure Captions

Fig. 1

Austenite grain growth kinetics after heating at ϕ=5°C/s to the isothermal measurement temperature. The experimental results and the lines representing the fit based on equation (7) are shown.

Fig. 2

Comparison of log normal distribution (solid lines) with experimental two-dimensional austenite grain size distribution at 1150°C after 60s (a) and 450s (b).

Fig. 3

Austenite isothermal grain growth kinetics obtained after heating at ϕ=100°C/s to the measurement temperature. The experimental results and the lines representing the fit based on equation (7) are shown.

Fig. 4

Austenite grain growth during continuous cooling from 1120 to 1000°C at 2°C/s.

Fig. 5

Comparison of the predictions from the statistical grain growth model (solid lines) with austenite isothermal grain growth kinetics occurring by normal growth for an initial heating rate, ϕ=5°C/s. The grain size is represented by the average value, D, according equation (5).

Fig. 6

Pinning parameter for the A36 steel for different heating rates, ϕ, to the measurement temperature.

Fig. 7

Comparison of experimentally observed limiting grain radius and those predicted from the pinning parameter employing Zener's criterion.

Fig. 8

Comparison of log normal distribution (solid lines) with experimental two-dimensional ferrite grain size distribution obtained after continuous cooling at a) $\varphi = 41°C/s$ and b) $\varphi = 58°C/s$.

Fig. 9

Final ferrite grain size as a function of cooling rate.

Fig. 10

Final ferrite grain size as a function of transformation start temperature during continuous cooling compared to calculations based on equations (19) and (20).

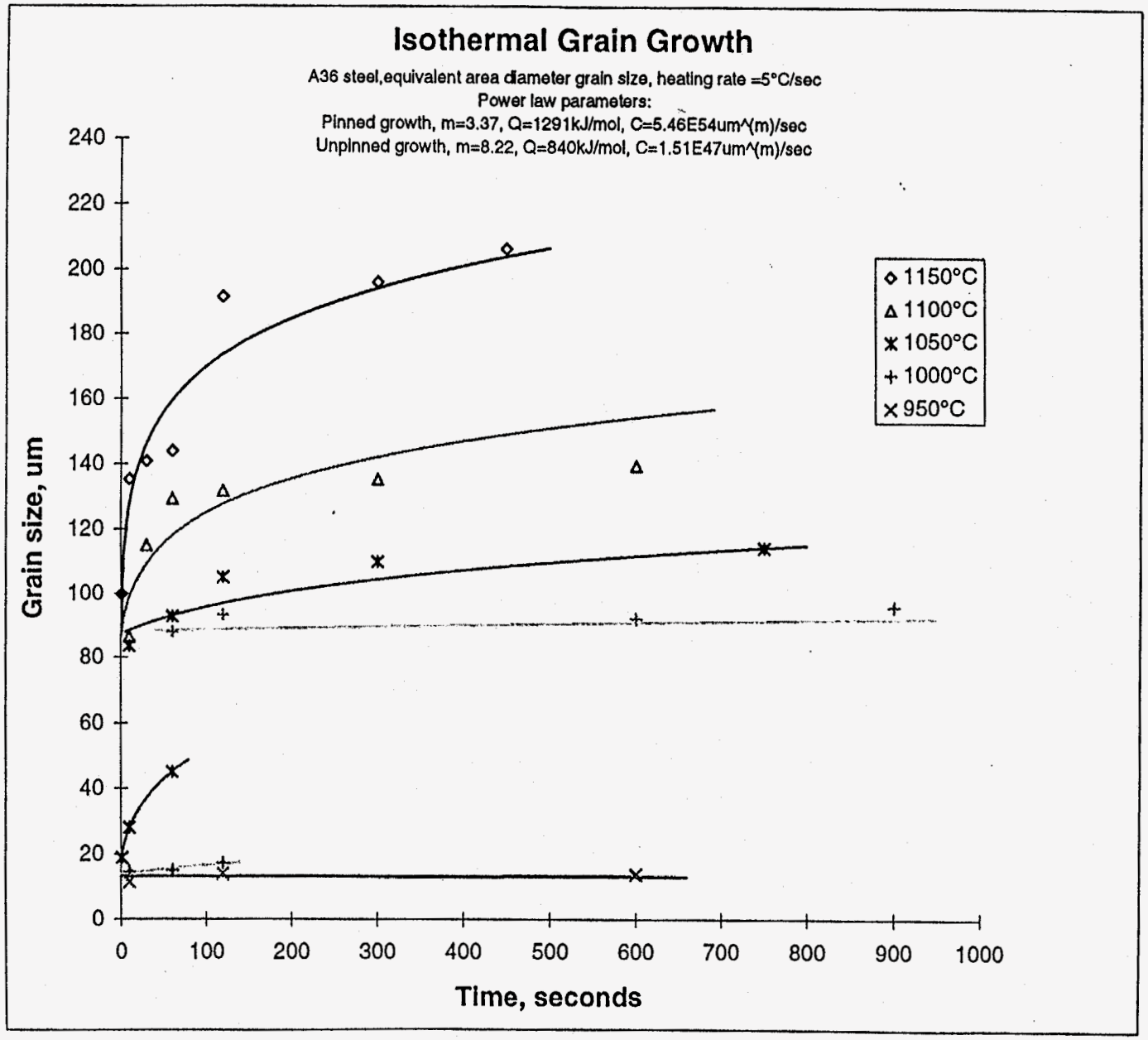
Isothermal Grain Growth
A36 steel,equivalent area diameter grain size, heating rate =5°C/sec
Power law parameters:
Pinned growth, m=3.37, Q=1291kJ/mol, C=5.46E54um^(m)/sec
Unpinned growth, m=8.22, Q=840kJ/mol, C=1.51E47um^(m)/sec
Grain size, um
Time, seconds
1150°C
1100°C
1050°C
1000°C
950°C
0
20
40
60
80
100
120
140
160
180
200
220
240
0
100
200
300
400
500
600
700
800
900
1000

Fig. 1

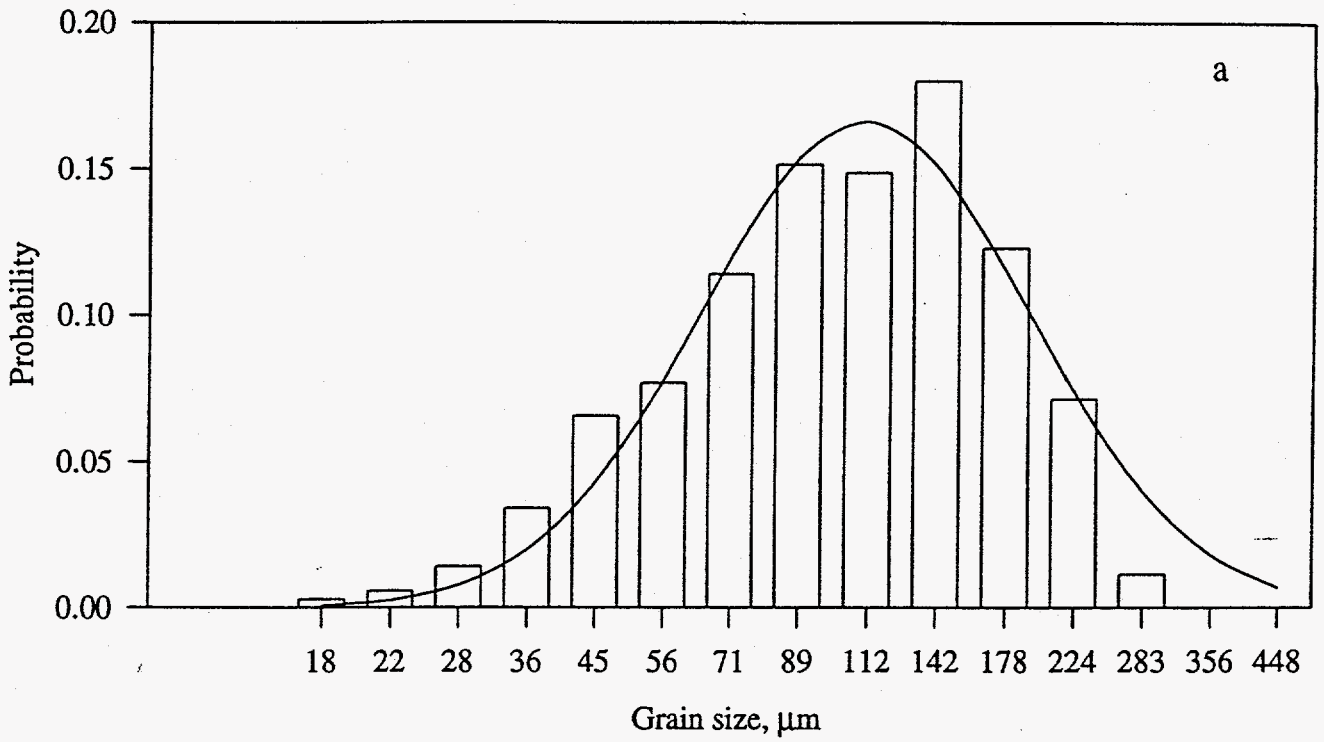
0.20
0.15
0.10
0.05
0.00
Probability
a
18 22 28 36 45 56 71 89 112 142 178 224 283 356 448
Grain size, µm

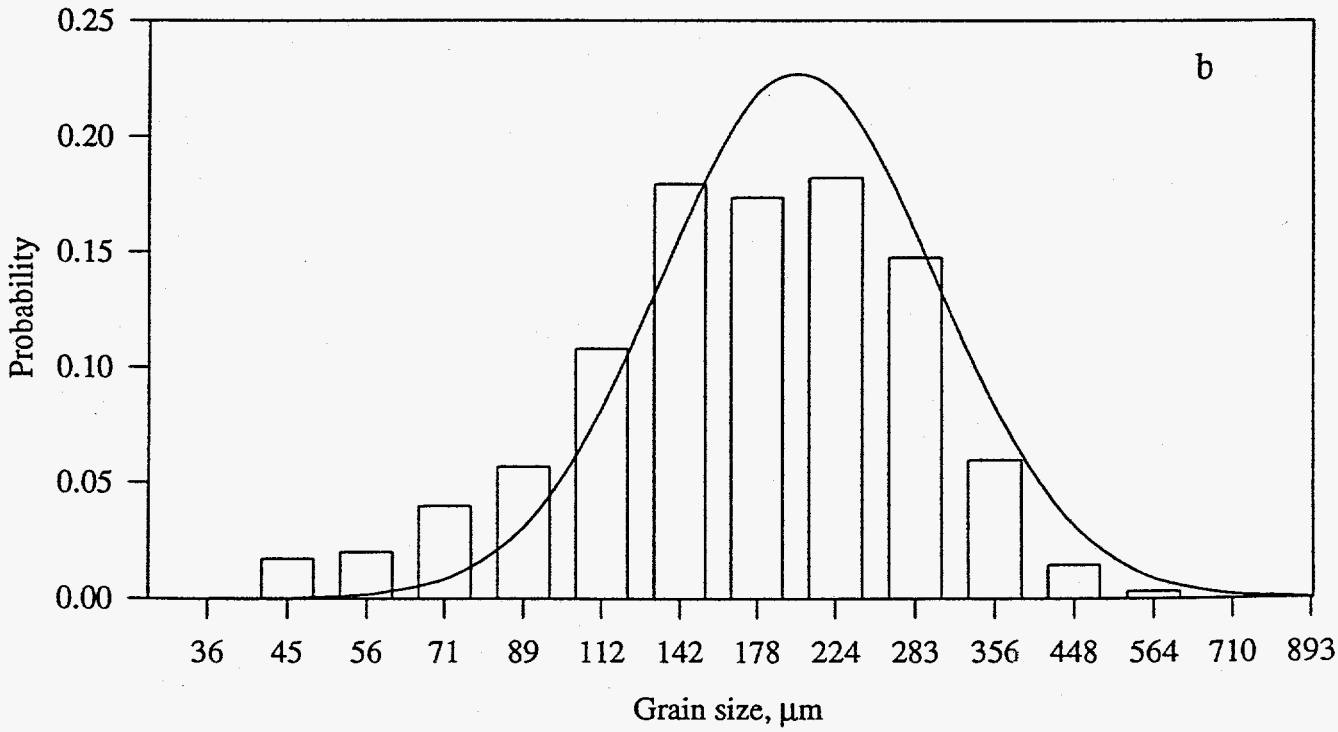
0.25
0.20
0.15
0.10
0.05
0.00
Probability
b
36 45 56 71 89 112 142 178 224 283 356 448 564 710 893
Grain size, µm

Fig. 2

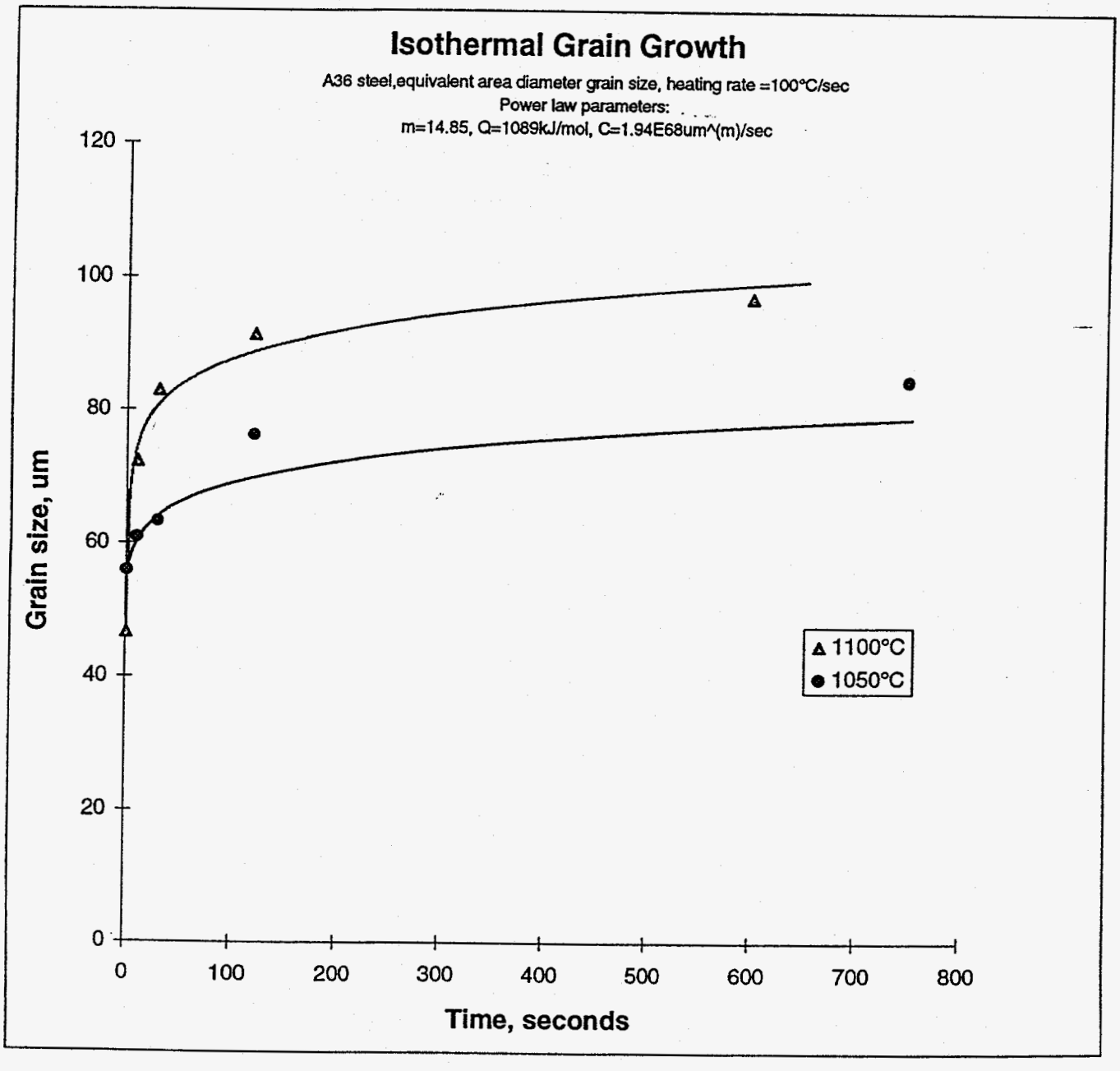
Isothermal Grain Growth
A36 steel,equivalent area diameter grain size, heating rate =100°C/sec
Power law parameters:
m=14.85, Q=1089kJ/mol, C=1.94E68um^(m)/sec
Grain size, um
120
100
80
60
40
20
0
0
100
200
300
400
500
600
700
800
Time, seconds
1100°C
1050°C

Fig. 3

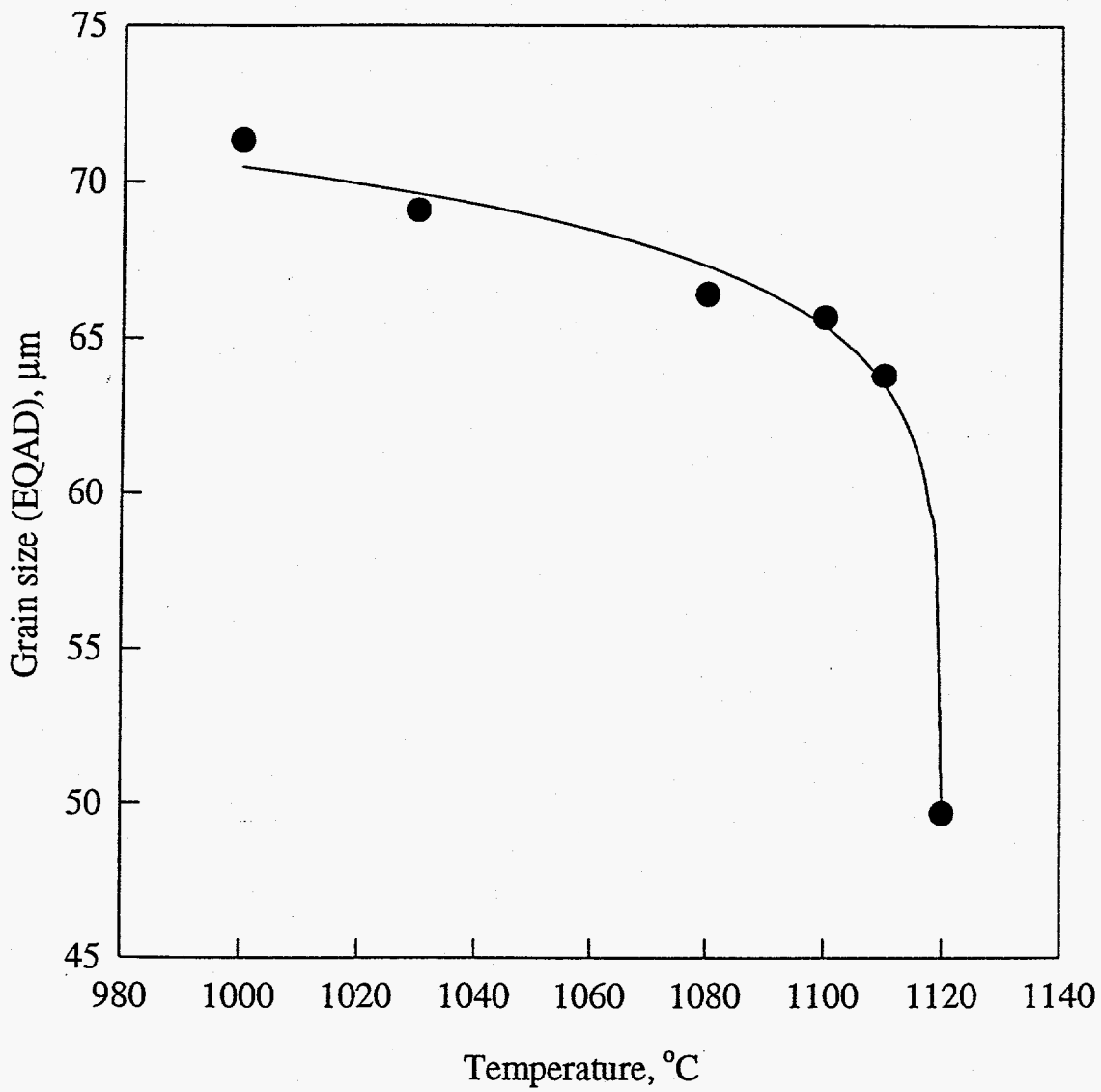
75
70
65
60
55
50
45
Grain size (EQAD), µm
980
1000
1020
1040
1060
1080
1100
1120
1140
Temperature, °C

Fig. 4

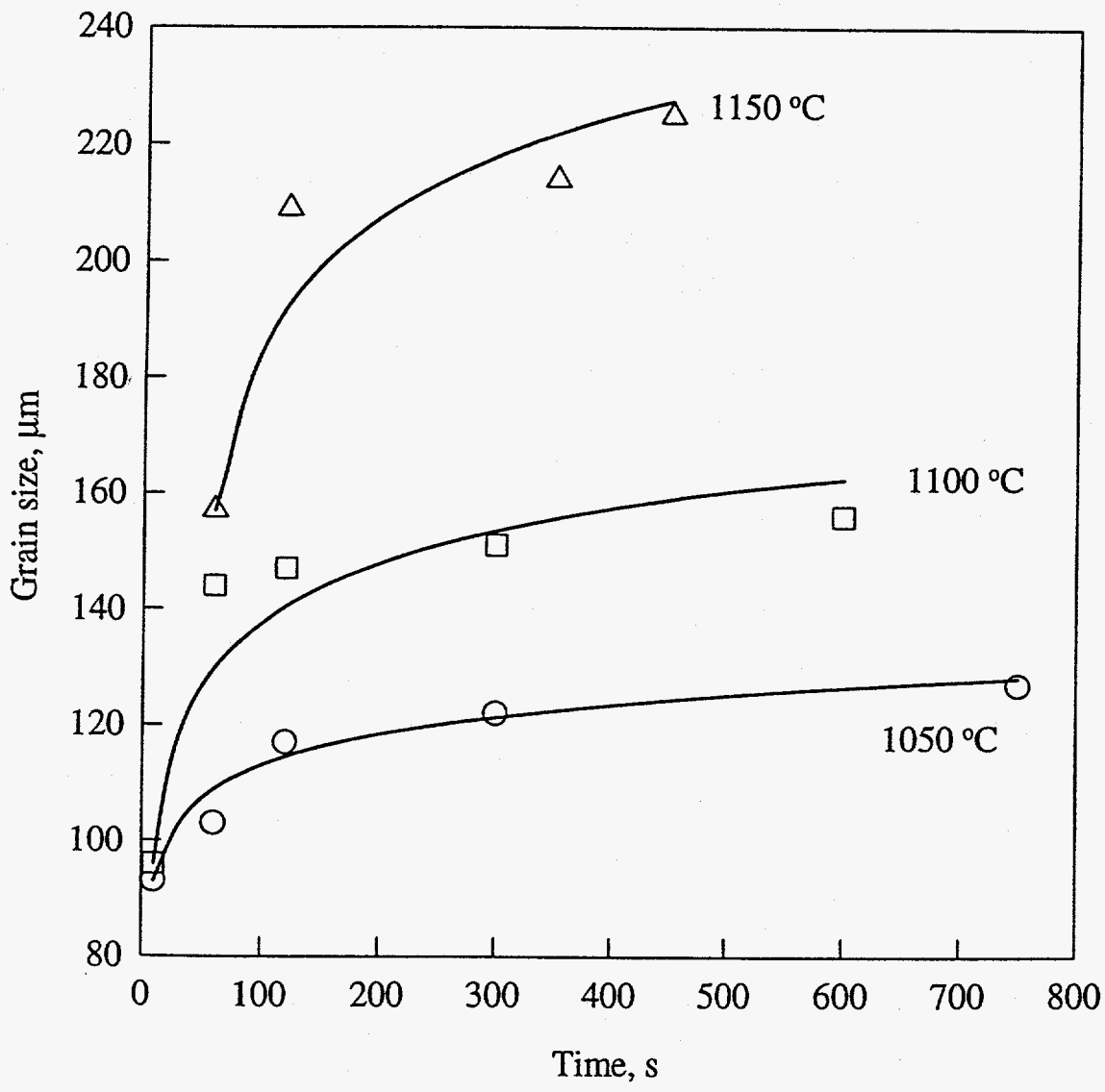
240
220
200
180
160
140
120
100
80
Grain size, μm
0
100
200
300
400
500
600
700
800
Time, s
1150 °C
1100 °C
1050 °C

Fig. 5

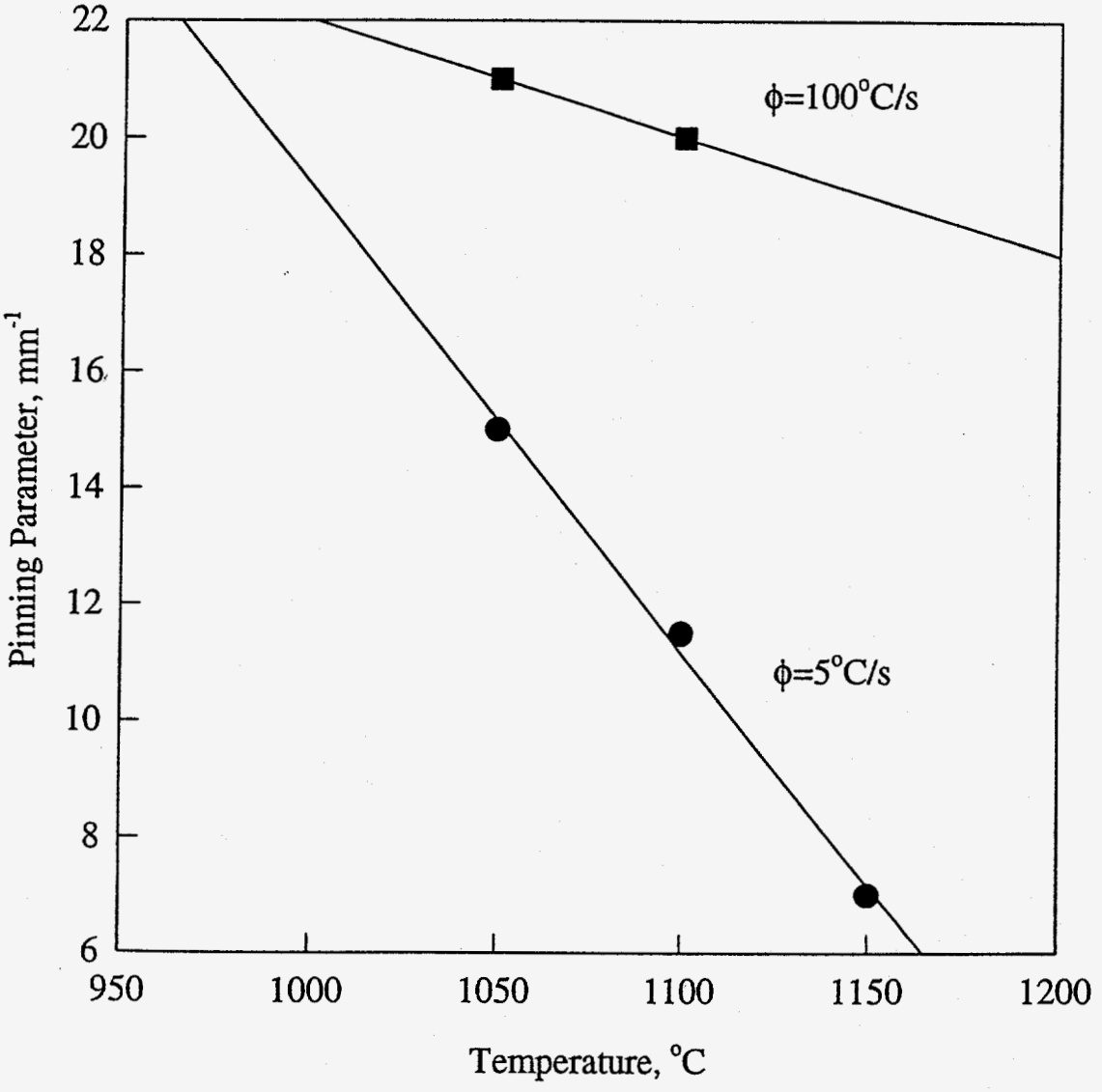
22
20
18
16
14
12
10
8
6
Pinning Parameter, mm-1
950
1000
1050
1100
1150
1200
Temperature, °C
ϕ=100°C/s
ϕ=5°C/s

Fig. 6

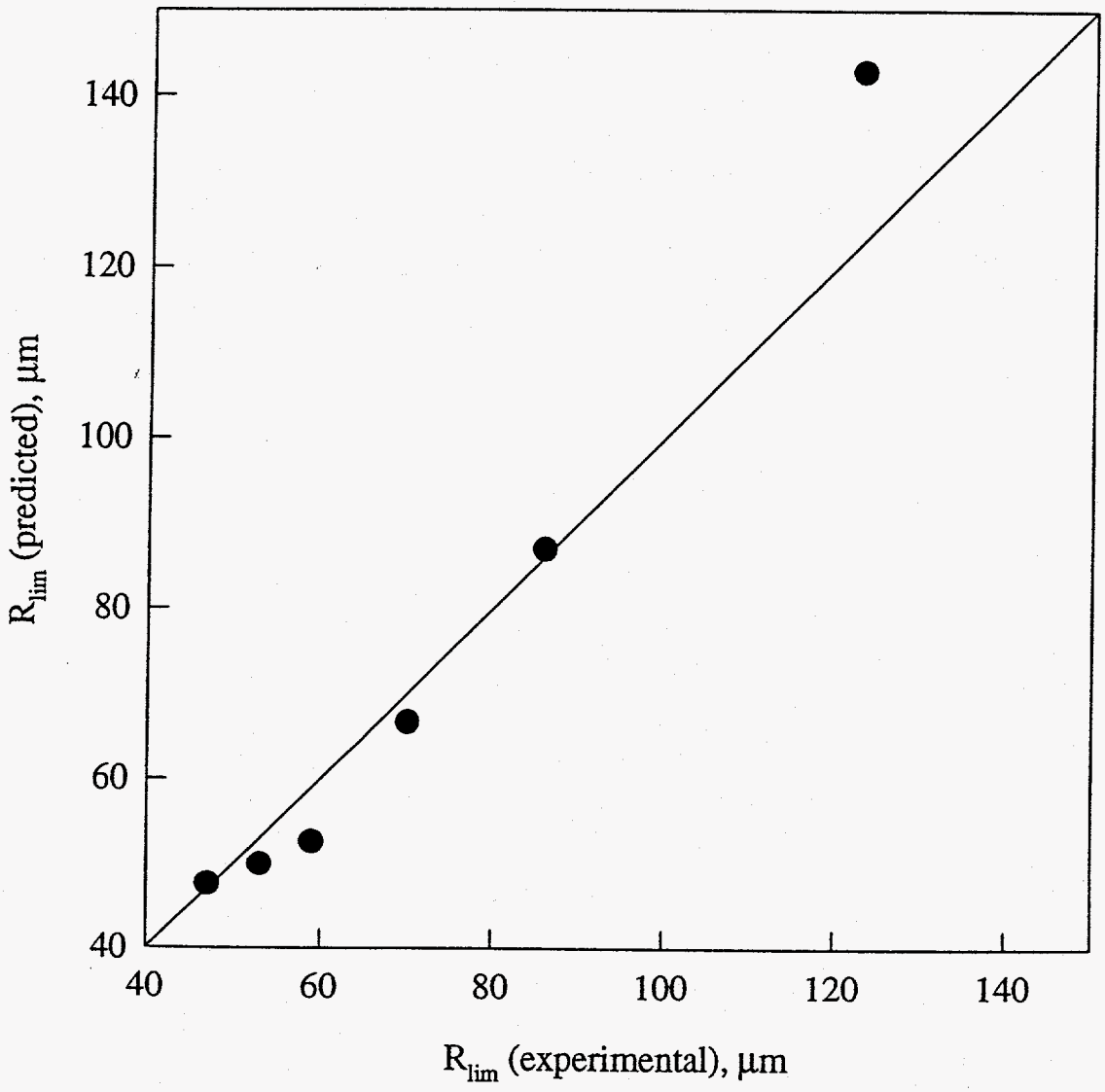
140
120
100
80
60
40
40
60
80
100
120
140
R_{lim} (predicted), µm
R_{lim} (experimental), µm

Fig. 7

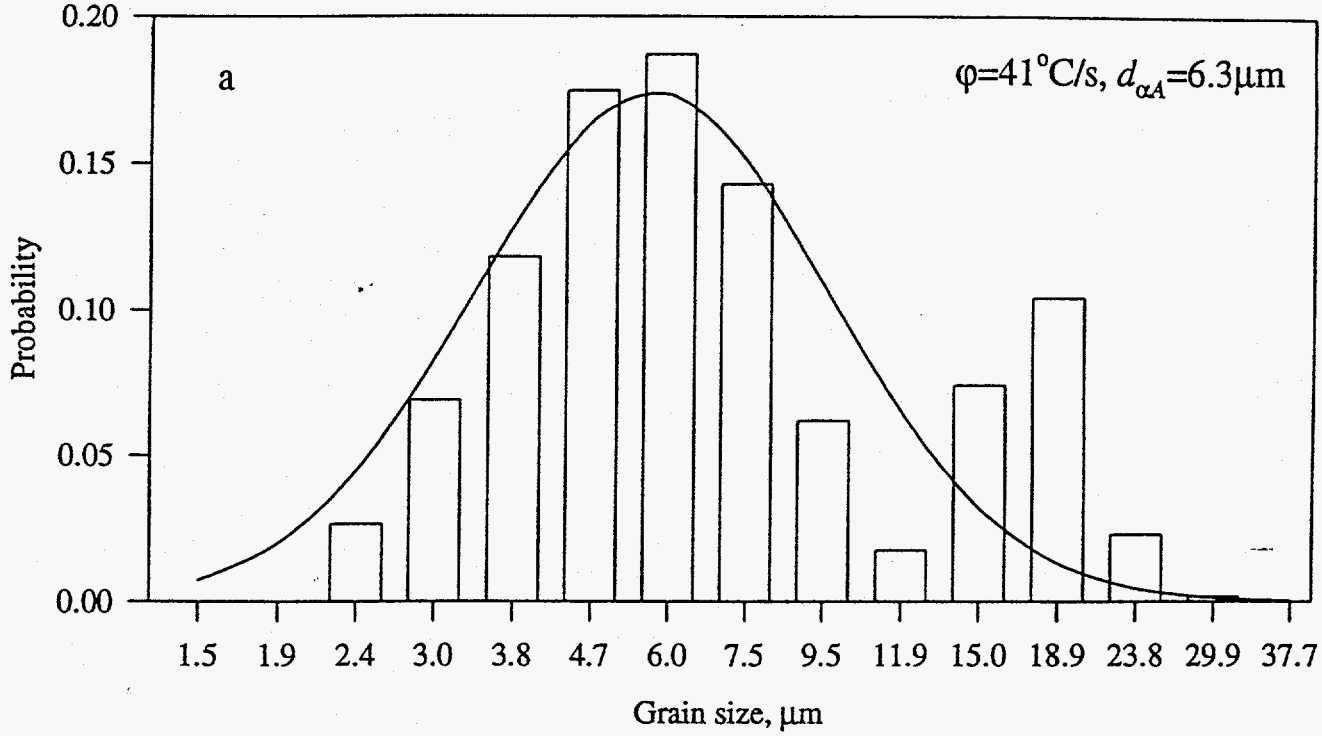
a
φ=41°C/s, $d_{\alpha A}$=6.3μm
Probability
0.20
0.15
0.10
0.05
0.00
1.5 1.9 2.4 3.0 3.8 4.7 6.0 7.5 9.5 11.9 15.0 18.9 23.8 29.9 37.7
Grain size, μm

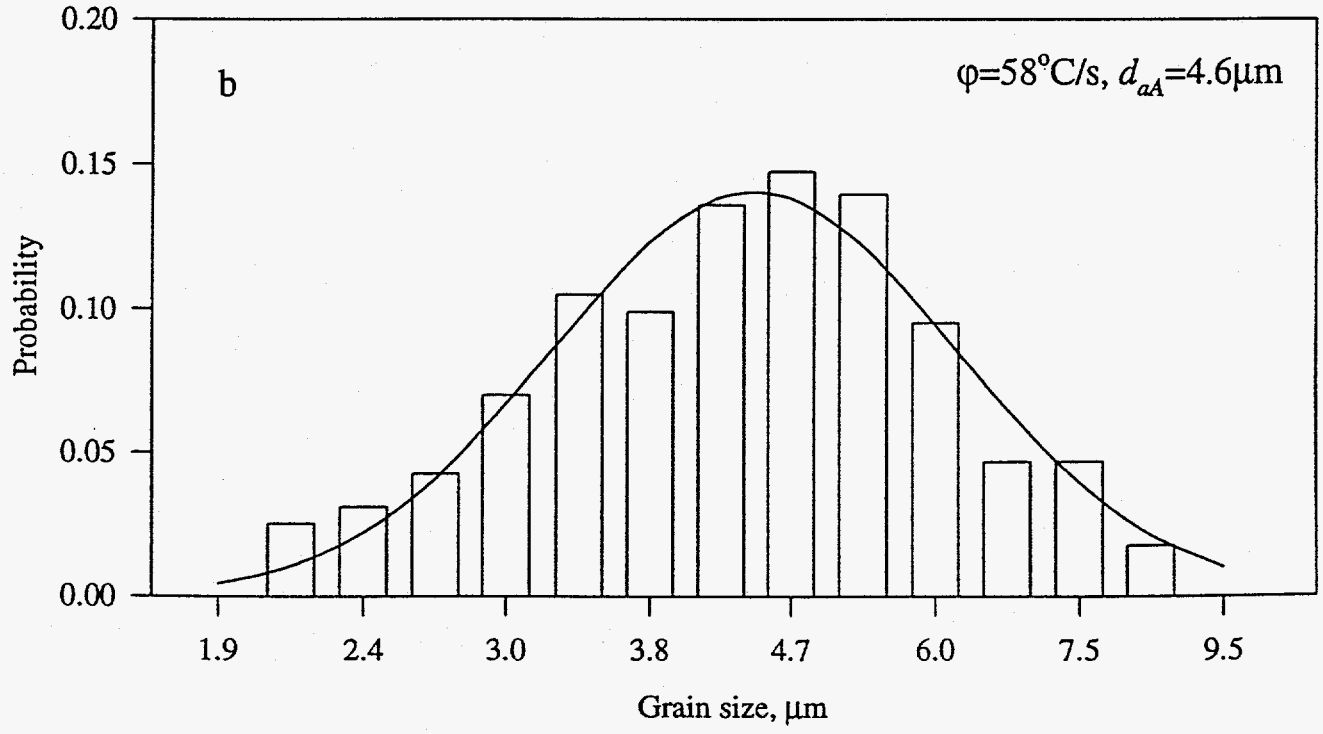
b
φ=58°C/s, d_{aA}=4.6μm
Probability
0.20
0.15
0.10
0.05
0.00
1.9 2.4 3.0 3.8 4.7 6.0 7.5 9.5
Grain size, μm

Fig. 8

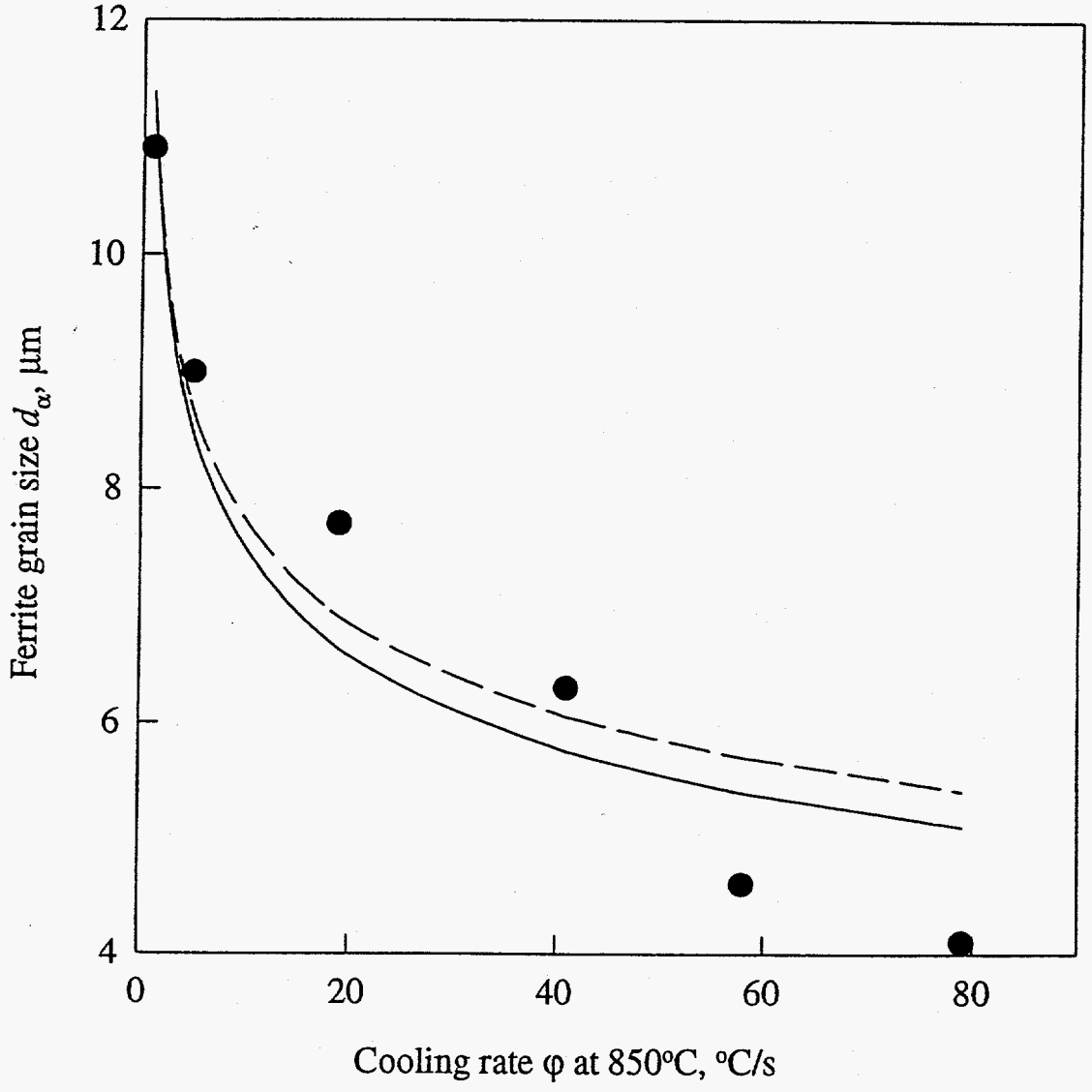
12
10
8
6
4
0
20
40
60
80
Ferrite grain size d_α, μm
Cooling rate φ at 850°C, °C/s

Fig. 9

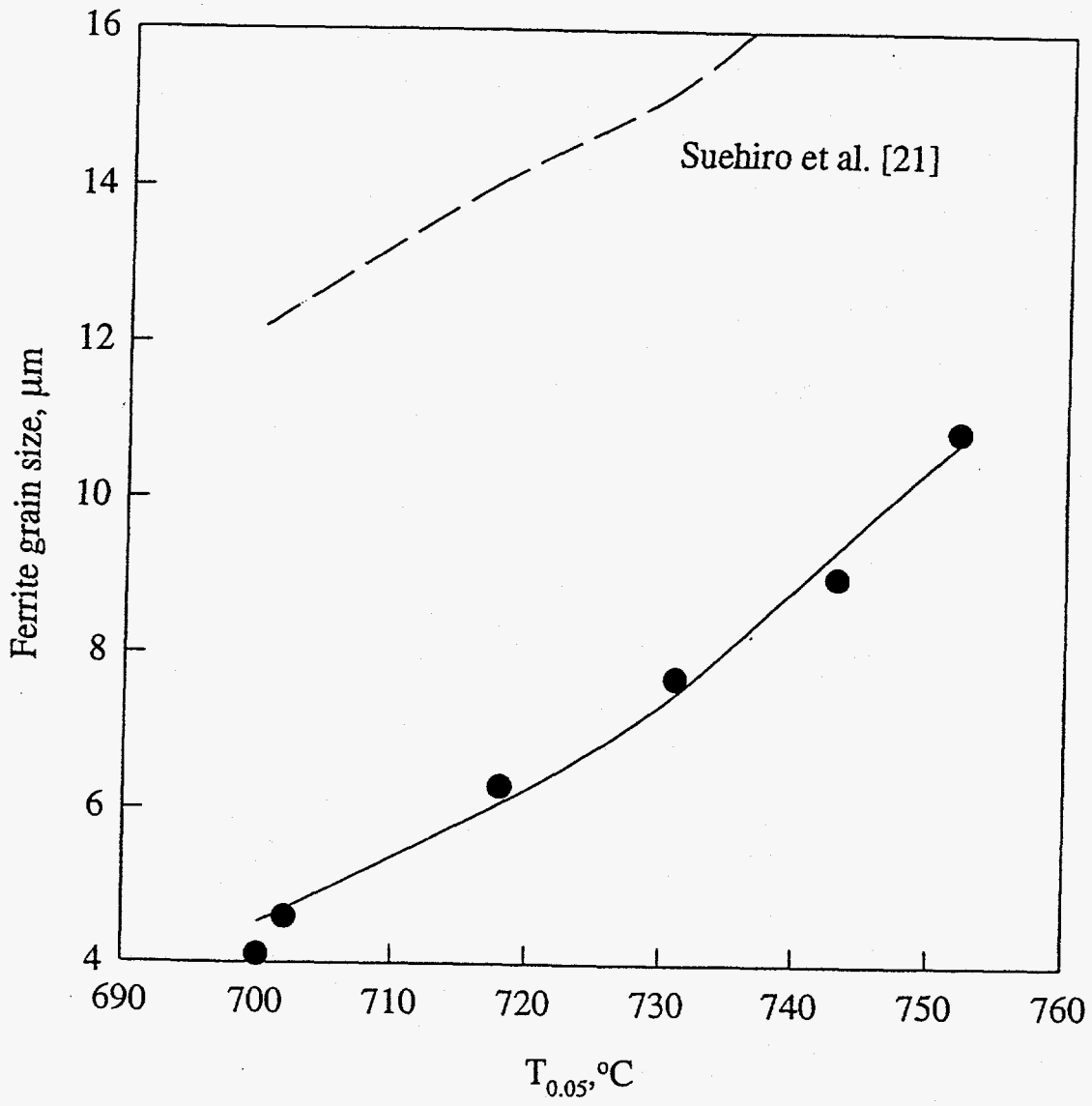

Fig. 10

DISCLAIMER